

# Photoinduced Formation Mechanism of the Thymine–Thymine (6–4) Adduct

Angelo Giussani,<sup>\*,†</sup> Luis Serrano-Andrés,<sup>†</sup> Manuela Merchán,<sup>†</sup> Daniel Roca-Sanjuán,<sup>\*,‡</sup> and Marco Garavelli<sup>\*,§</sup>

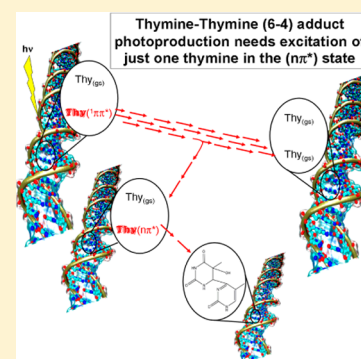
<sup>†</sup>Instituto de Ciencia Molecular, Universitat de València, Apartado 22085, ES-46071 Valencia, Spain

<sup>‡</sup>Department of Chemistry – Ångström, Theoretical Chemistry Program, Uppsala University, Box 518, 75120 Uppsala, Sweden

<sup>§</sup>Dipartimento di Chimica “G. Ciamician”, Università di Bologna, Via Selmi 2, 40126 Bologna, Italy

## S Supporting Information

**ABSTRACT:** The photoinduced mechanism leading to the formation of the thymine–thymine (6–4) photoproduct has been studied by using the CASPT2//CASSCF approach over a dinucleotide model in vacuo. Following light absorption, localization of the excitation on a single thymine leads to fast singlet–triplet crossing that populates the triplet  $^3(n\pi^*)$  state of thymine. This state, displaying an elongated  $C_4=O$  bond, triggers (6–4) dimer formation by reaction with the  $C_5=C_6$  double bond of the adjacent thymine, followed by a second intersystem crossing, which acts as a gate between the excited state of the reactant and the ground state of the photoproduct. The requirement of localized excitation on just one thymine, whose main decay channel (by radiationless repopulation of its ground state) is nonphotochemical, can rationalize the experimentally observed low quantum yield of formation for the thymine–thymine (6–4) adduct.



## INTRODUCTION

Two major photoproducts are obtained as a consequence of ultraviolet (UV) irradiation of pyrimidine nucleobases, cyclobutane pyrimidine dimers (Pyr<>Pyr) and pyrimidine–pyrimidone (6–4) adducts.<sup>1,2</sup> Due to their mutagenic properties, the formation of these molecules in DNA by the photoinduced reaction of two adjacent pyrimidine nucleobases from the same strand constitutes a photolesion of major impact associated with prolonged light exposure of living organisms. Probably due to its higher yield of formation in cellular DNA,<sup>3</sup> the mechanism of production of Pyr<>Pyr dimers has been the subject of many different theoretical<sup>4–7</sup> and experimental studies,<sup>8–11</sup> while little is known about the processes that pyrimidine nucleobases undergo from UV absorption to pyrimidine–pyrimidone (6–4) adduct formation.<sup>12–15</sup> Efforts have been recently devoted to the description of the repair mechanism that reverses the (6–4) photodamage.<sup>16–18</sup> It is well accepted that (6–4) production takes place via oxetane (Ox) or azedine intermediates, their formation being the actual photoactivated part of the global process, followed by thermal ring opening.<sup>1</sup> In the case of two thymine molecules, the intermediate produced during UV irradiation is an Ox structure (see Figure 1) caused by the reaction of  $C_5=C_6$  and  $C_4=O$  double bonds belonging to different moieties. The photochemical addition of carbonyl compounds to alkenes to form Ox's, known as the Paternò–Büchi reaction,<sup>19</sup> is usually assumed to take place via the triplet  $^3(n\pi^*)$  excited state of the carbonyl compound, although the reaction can also proceed along the singlet manifold.<sup>20</sup> Here, we have employed an ab

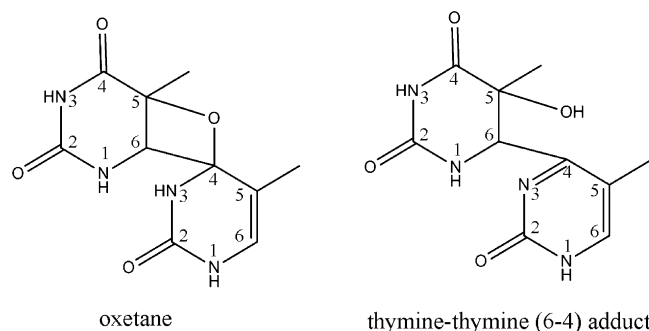


**Figure 1.** Structure of the thymine–thymine (6–4) adduct and its Ox precursor.

initio CASPT2//CASSCF approach to map the photochemically relevant potential energy hypersurfaces (PEHs) responsible for the photoinduced formation of the thymine–thymine (6–4) adduct (see Figure 1). The mechanistic key elements driving the global photoreaction have been elucidated.

## THEORETICAL METHODS

The present study has been performed by using the well-tested CASPT2//CASSCF methodology<sup>21–24</sup> as implemented in the MOLCAS 7.4 software.<sup>25</sup> Optimized structures and minimum

Received: July 20, 2012

Revised: December 26, 2012

Published: January 23, 2013

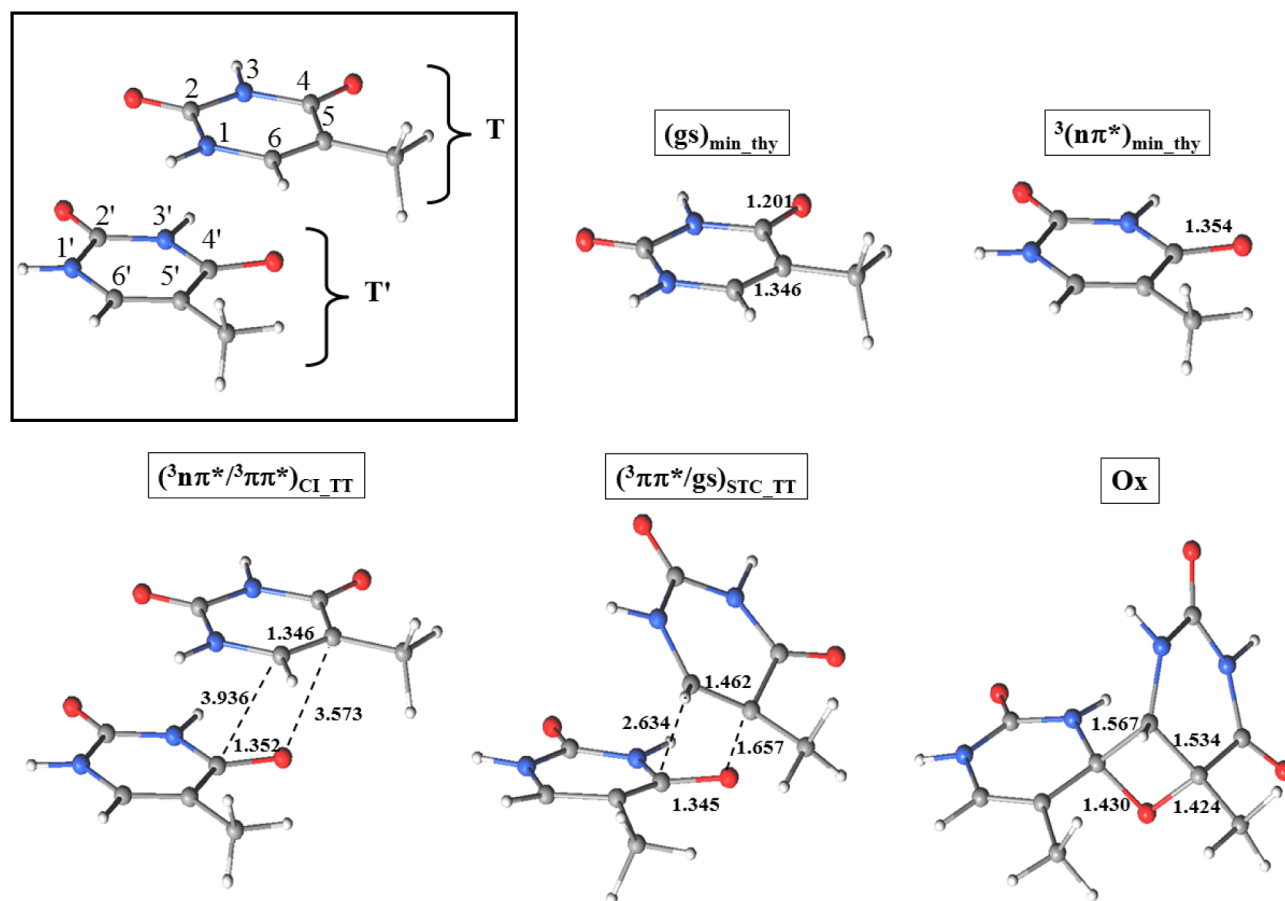


**Figure 2.** Main structures involved in the mechanism for the photoproduction of the Ox intermediate. Bond lengths are reported in Ångstroms. In the inset, atom and nucleobase labeling are shown.

energy paths (MEPs) have been then calculated at the multiconfigurational CASSCF level, and at the geometries so obtained, dynamic correlation effects have been taken into account by performing second-order multiconfigurational CASPT2 calculations. All computations have been carried out by imposing no restrictions on the symmetry of the molecule ( $C_1$  symmetry). Basis sets of the atomic natural orbital (ANO) of S-type contracted to  $C, N, O[3s, 2p, 1d]/H[2s, 1p]$  have been employed.<sup>26</sup> The active space in the CASSCF and CASPT2 calculations is composed of 6 electrons and 6 orbitals for one thymine nucleobase and 12 electrons and 12 orbitals for the dimer system formed by two thymine molecules. Within the CASPT2 calculations, an imaginary level-shift correction of 0.2 au has been used in order to avoid the presence of intruder states. The CASPT2 standard zeroth-order Hamiltonian has been employed as originally implemented.<sup>22</sup> The core orbitals have been frozen in the CASPT2 calculations. Such a CASPT2 approach has been validated during the last decades in many different studies on organic molecules, providing a correct prediction, description, and interpretation of the photophysical and photochemical experimental data.<sup>27–29</sup> CIs have been computed by using the restricted Lagrange multipliers technique as included in the MOLCAS 7.4 package in which the lowest-energy point is obtained under the restriction of degeneracy between the two considered states.<sup>25</sup> Additional computational details can be found in the Supporting Information, where the methods employed for the calculation of the spin–orbit coupling (SOC) and for the evaluation of the basis set superposition error (BSSE) are described.

## RESULTS AND DISCUSSION

It is well recognized that DNA is a very flexible structure. Its conformation at the time of light irradiation has been proven to be of primary importance in determining the way in which the absorbed energy can be released by the system.<sup>4,8</sup> In particular, the degree of stacking and the distance between the nucleobases strongly influence whether the excitation will be localized on a single nucleobase or delocalized among them. In the former, the first process that follows UV irradiation is related to the photophysics of a single nucleobase. According to the present results, it is predicted that (6–4) adduct formation from the stacked thymine–thymine (TT) system is triggered by a local geometry that allows localization of the excitation on a single thymine molecule, whose photoresponse represents the initial step of the global photoreaction.

The minimum reaction path of thymine starting at the ground-state optimized geometry on the brightest  $^1(\pi\pi^*)$  singlet excited state, hereafter  $(gs)_{\min\_thy}$  is barrierless, leading to an ethene-like conical intersection with the ground state, determining the photostability of thymine.<sup>30,31</sup> Along this main decay path, a singlet–triplet intersystem crossing region has been found, which in the present work is coincident with the  $(gs)_{\min\_thy}$  geometry, hereafter denoted also as  $(^1\pi\pi^*/^3\pi\pi^*)_{STC\_thy}$ . Thus, part of the population of the bright  $^1(\pi\pi^*)$  might be transferred to the  $^3(n\pi^*)$  state, owing also to the significant spin–orbit coupling computed at this point ( $14.5\text{ cm}^{-1}$ ). Once the  $^3(n\pi^*)$  state is populated, it evolves to a minimum structure, denoted as  $^3(n\pi^*)_{\min\_thy}$  (see Figure 2),

characterized by an elongated  $C_4=O$  bond (1.354 Å). Such a structural condition is a key driver for the global photoreaction because it causes a partial loss of the double bond character of the  $C_4=O$  bond and consequently favors the reaction of the carbonyl group with an adjacent carbon–carbon double bond. From the  $^3(n\pi^*)_{\text{min\_thy}}$  region, the presence of a nearby conical intersection between the  $^3(n\pi^*)$  and  $^3(\pi\pi^*)$  states allows the relaxation of the thymine system to a minimum of the  $^3(\pi\pi^*)$  state, which might finally decay to the ground state by surmounting a small barrier that leads to an intersystem crossing region.<sup>31,32</sup>

For a nonhighly stacked TT system, the photophysical response of the bright excited state  $^1(\pi\pi^*)$  localized on a single nucleobase is expected to be the same as the one described above for the isolated thymine molecule. Consequently, the TT system should decay via a radiationless process to the ground state, and, to a less extent, population of the  $^3(n\pi^*)$  state should take place. In order to validate such a hypothesis, we have studied the potential energy hypersurface between the TT system in its B-DNA conformation [ $(gs)_{\text{B-DNA}}$  hereafter] and the same structure in which one thymine (denoted as T') has been replaced with the excited  $^3(n\pi^*)_{\text{min\_thy}}$  geometry and the other monomer (denoted as T) has been left as in its ground-state conformation (see Figure 2). The last geometry will be named  $^3(n\pi^*)_{\text{min\_TT}}$ . At the  $(gs)_{\text{B-DNA}}$  structure, the brightest singlet excited states are indeed localized on the T' and T moieties, respectively (see Figure S2, Supporting Information). As for one thymine, the  $(gs)_{\text{min\_B-DNA}}$  structure constitutes a single triplet crossing region between the localized  $^1(\pi\pi^*)$  and the  $^3(n\pi^*)$  states; therefore, it will be also denoted as  $(^1\pi\pi^*/^3n\pi^*)_{\text{STC\_B-DNA}}$ . The plausibility of our hypothesis is confirmed by the presence of a barrierless path between the  $(gs)_{\text{B-DNA}}$  –  $(^1\pi\pi^*/^3n\pi^*)_{\text{STC\_B-DNA}}$  and  $^3(n\pi^*)_{\text{min\_TT}}$  structures and because their energies are comparable to the values for  $(gs)_{\text{min\_thy}}$  and  $^3(n\pi^*)_{\text{min\_thy}}$ , respectively (see Tables S1 and S2, Supporting Information). The  $^3(n\pi^*)_{\text{min\_TT}}$  is almost degenerate with a conical intersection between the localized  $^3(n\pi^*)$  and  $^3(\pi\pi^*)$  states, hereafter  $(^3n\pi^*/^3\pi\pi^*)_{\text{CL\_TT}}$  (see Figure 2), responsible for the decay to the  $^3(\pi\pi^*)$  state. Once in the  $(^3n\pi^*/^3\pi\pi^*)_{\text{CL\_TT}}$  region, the  $^1(\pi\pi^*)$  state is clearly far in energy (see Table S2, Supporting Information), which discards a further evolution of the system on the singlet manifold.

The  $(^3n\pi^*/^3\pi\pi^*)_{\text{CL\_TT}}$  structure is connected with an intersystem crossing region  $(^3\pi\pi^*/gs)_{\text{STC\_TT}}$  on the potential energy hypersurface of the  $^3(\pi\pi^*)$  state by surmounting a small barrier of 0.20 eV. Along this path, the originally localized excitation that characterized the  $^3(\pi\pi^*)$  state at the  $(^3n\pi^*/^3\pi\pi^*)_{\text{CL\_TT}}$  geometry becomes increasingly delocalized on the adjacent thymine and finally describes a charge-transfer state from the T to the T' nucleobase at the  $(^3\pi\pi^*/gs)_{\text{STC\_TT}}$  structure (see Figures S4–S8, Supporting Information). The very same excitation characterizing the  $T_1$  state at this intersystem crossing region also describes the  $S_1$ – $^1(\pi\pi^*)$  state, which is now degenerate with both the ground and the  $^3(\pi\pi^*)$  state (see Table S2, Supporting Information). The  $(^3\pi\pi^*/gs)_{\text{STC\_TT}}$  can be consequently considered a region of triple crossing, involving the  $S_0$ ,  $S_1$ , and  $T_1$  surfaces. A similar conical intersection between the ground and the lowest singlet excited state was previously described by Blancafort and Migani, although a connected path from the absorbed excited state to such a conical intersection was not identified.<sup>12</sup> The  $(^3\pi\pi^*/gs)_{\text{STC\_TT}}$  geometry is of paramount importance in the formation mechanism of the thymine–thymine (6–4) adduct

because it is connected through an almost barrierless path with the ground state of the Ox intermediate and consequently can funnel the system from the excited-state reactant to the ground-state photoproduct. Once the system reaches the  $(^3\pi\pi^*/gs)_{\text{STC\_TT}}$  region, it would finally decay to the Ox geometry, concluding the photoactivated part of the mechanism that gives rise to the thymine–thymine (6–4) adduct. The highly unstable Ox intermediate is subsequently converted into the thymine–thymine (6–4) adduct through thermal migration of the 4-exocyclic keto group of the T' nucleobase to the C5 position of the T moiety.<sup>1</sup> In the  $(^3\pi\pi^*/gs)_{\text{STC\_TT}}$  structure, the  $C_4=O$  bond distance of the T' fragment is equal to 1.345 Å, the  $C_5=C_6$  bond of T is elongated, reaching a bond length of 1.462 Å, and the O– $C_5$  bond present in the Ox intermediate is almost formed (1.657 Å). The  $(^3\pi\pi^*/gs)_{\text{STC\_TT}}$  is characterized by a biradical character, having the unpaired electrons located on the  $C_6$ ,  $C_4'$ , and  $C_6'$  atoms, similar to the intermediate intersystem crossing regions for the formation of cyclobutane pyrimidine dimers along the triplet manifold.<sup>6</sup>

The population of the  $^3(n\pi^*)$  state through the  $(^1\pi\pi^*/^3n\pi^*)_{\text{STC\_B-DNA}}$  intersystem crossing region constitutes the starting point of the above description. According to previous studies, an internal conversion process toward the localized  $^1(n\pi^*)$  state can also be expected because for the isolated thymine system, an accessible conical intersection between the  $^1(\pi\pi^*)$  and  $^1(n\pi^*)$  states has been actually described and because the PEHs of singlet and triplet  $n\pi^*$  states have been proven to run parallel.<sup>31</sup> In the present study, the energies of the  $^1(n\pi^*)$  state along the path connecting the Franck–Condon and  $(^3n\pi^*/^3\pi\pi^*)_{\text{CL\_TT}}$  regions have been determined. The results show that also for the TT system, the PEHs of the singlet and triplet  $n\pi^*$  states are almost coincident (see Table S2, Supporting Information). On the basis of these results, and for the mentioned reasons, it seems reasonable to expect that the  $^1(n\pi^*)$  state might be populated from the  $^1(\pi\pi^*)$  state and subsequently evolve to the  $^3(n\pi^*)_{\text{min\_TT}}$  structure. Furthermore, the  $(^3n\pi^*/^3\pi\pi^*)_{\text{CL\_TT}}$  conical intersection represents also a singlet–triplet crossing region between the  $^1(n\pi^*)$  and the  $^3(\pi\pi^*)$  states ( $\Delta E = 0.02$  eV, SOC = 5.2  $\text{cm}^{-1}$ ), which consequently allows the system in the  $^1(n\pi^*)$  state at the  $^3(n\pi^*)_{\text{min\_thy}}$  structure to decay to the  $^3(\pi\pi^*)$  state and evolve to the  $(^3\pi\pi^*/gs)_{\text{STC\_TT}}$  geometry.

As previously pointed out, the  $(^3\pi\pi^*/gs)_{\text{STC\_TT}}$  singlet–triplet crossing structure from which the system decays to the Ox geometry represents also a conical intersection between the lowest singlet states. At this point, both the  $S_1$  and  $T_1$  states have a charge-transfer character, mainly described by an excitation from the T to the T' nucleobase. It would consequently be interesting to study the possibility of populating the  $(^3\pi\pi^*/gs)_{\text{STC\_TT}}$  region along the singlet manifold and to analyze the role of the charge-transfer states in the overall photoprocess. According to the above outcomes, through the bright  $^1(\pi\pi^*)$  and then the  $^1(n\pi^*)$  states, it could be possible to reach the  $^3(n\pi^*)_{\text{min\_thy}}$  reactive structure, which constitutes the starting point of the reaction between the two thymine molecules. From such a region, the  $^1(n\pi^*)$  state cannot further decay along the singlet manifold because all other singlet states are far above in energy. On the basis of these results, we then conclude that the presented mechanism cannot take place entirely along the singlet states. The existence of a different connected path along the singlet manifold that from the brightest states leads to the  $(^3\pi\pi^*/gs)_{\text{STC\_TT}}$  structure

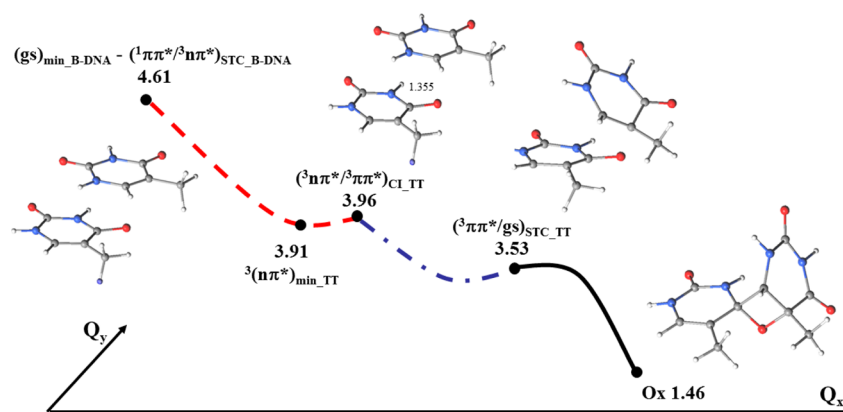


**Figure 3.** Proposed scheme for the photoinduced formation mechanism of the Ox precursor of the thymine–thymine (6–4) adduct. The reported energies (eV) have been calculated at the CASPT2+CP-BSSE//CASSCF(12,12)/ANO-S C,N,O [3s,2p,1d]/H[2s1p] level with respect to two isolated ground-state thymine molecules. Dashed red, dash–dot–dash blue, and solid dark lines indicate the evolution of the system on the  $^3(n\pi^*)$ ,  $^3(\pi\pi^*)$ , and ground state, respectively. The  $Q_x$  coordinate is related mainly to the  $C_4'O$  bond stretching, coupled with the variation of the main intermolecular distance.  $Q_y$  represents the remaining degree of freedom.

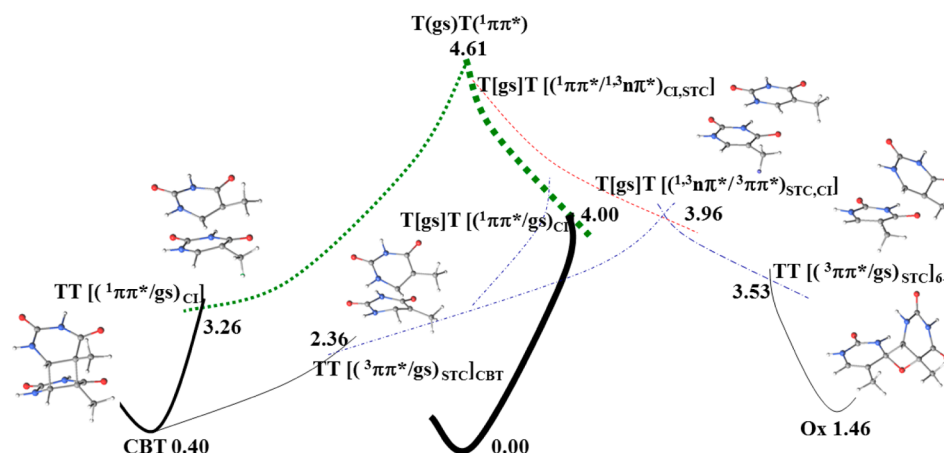


**Figure 4.** Global view for the photophysical response of the TT system under direct UV absorption based on the present and previous studies.<sup>5,6,30,31</sup> The reported energies (eV) have been calculated at the CASPT2+CP-BSSE//CASSCF(12,12)/ANO-S C,N,O [3s,2p,1d]/H[2s1p] level with respect to two isolated ground-state thymine molecules. Dotted green, dash–dot blue, and solid dark lines indicate the evolution of the system on the  $^1(\pi\pi^*)$ ,  $^3(\pi\pi^*)$ , and ground state, respectively. Dashed red lines indicate the evolution along both the  $^3(n\pi^*)$  and  $^1(n\pi^*)$  states. The thickness of the lines is an indicator of the probability of the path.

has not been computationally found. Blancafort and Migani, who have previously described a similar conical intersection, have correlated such a region with a high-lying charge-transfer state described in the B-DNA geometry as the S5 state.<sup>12</sup> Even if the hypothesis may be considered plausible, still a connected path to the conical region has not been provided. Another point regarding the importance of charge-transfer states in the global photoreaction, also highlighted in ref 12, is that at the B-DNA geometry, they are well above the brightest ones in energy. Consequently, although a connected path along the charge-transfer state could exist, it would remain to clarify how it can be populated from the brightest states.

On the basis of the current results, we can depict the following scheme for the formation mechanism of the Ox precursor, which can be divided in two main steps (see Figure 3). To activate the reaction between the carbonyl group of T' and the carbon–carbon double bond of T, the T' must be in a favorable molecular form. According to our outcomes, this structure is  $^3(n\pi^*)_{\text{min\_thy}}$ , which is in fact characterized by a considerable elongation of the carbonyl double bond. In the first step of the global mechanism, the excitation would be

localized on just one thymine and corresponds to the population of the  $^3(n\pi^*)_{\text{min\_thy}}$  geometry for the T' nucleobase, which depends on the actual geometry of the system at the time of light irradiation and on the efficiency of the intersystem crossing process through the  $(^1\pi\pi^*/^3n\pi^*)_{\text{STC\_thy}}$ . If the TT system absorbs the UV radiation in a conformation characterized by a relatively large separation between the two nucleobases, the excitation could remain localized on a single thymine. Once the  $^1(\pi\pi^*)$  state of T' is populated, the efficiency of the global process would be modulated by the effectiveness of the intersystem mechanism to the  $^3(n\pi^*)$  state. The second step of the global mechanism is the reaction of the excited T' with T along the presented pathway from the  $^3(n\pi^*)_{\text{min\_TT}}$  geometry to the Ox structure mediated by the presence of the  $(^3n\pi^*/^3\pi\pi^*)_{\text{CI\_TT}}$  conical intersection and the  $(^3\pi\pi^*/\text{gs})_{\text{STC\_TT}}$  intersystem crossing region. The efficiency of the second step is determined by the effectiveness of an intersystem mechanism with the ground state, competing with relaxation processes characterizing the photophysics of a single thymine triplet state.<sup>31</sup> The decay through the intersystem



crossing region is consequently an additional limiting factor of the global photoreaction.

As previously pointed out, the first described step of the global photoreaction might be mediated by the  $^1(n\pi^*)$  state because the  $^3(n\pi^*)_{\text{min\_TT}}$  reactive structure is expected to be populated also along such a state. From this situation, the system can subsequently decay through the second step of the described mechanism because the accessible  $(^3n\pi^*/^3\pi\pi^*)_{\text{CI\_TT}}$  geometry constitutes also a singlet–triplet crossing region between the  $^1(n\pi^*)$  and the  $^3(\pi\pi^*)$  states.

These nonadiabatic relaxation processes to the  $n\pi^*$  states are less efficient than the main decay of the thymine driven by the  $^1(\pi\pi^*)$  state. Hence, the population of the  $^{1,3}(n\pi^*)$  states required in the mechanism of (6–4) adduct formation can be considered as a limiting factor of the photoreaction.

Finally, combining the present results on the formation of the 6–4 adduct and our previous findings on the cyclobutane thymine dimer (CBT) photoproduction<sup>5,6</sup> and the energy decay paths found in the isolated T nucleobase,<sup>30,31</sup> we are in the position to provide a global view for the photophysical response of the TT system under direct UV absorption (see Figure 4), at least for our model system in vacuo. From the bright  $^1(\pi\pi^*)$  excited state, the system might undergo three main decay paths, repopulation of the ground state, CBT formation, and thymine–thymine (6–4) adduct production. The deactivation process followed by the system is initially and primarily controlled by the conformation at the time of light irradiation, which determines if the excitation will delocalize over the two nucleobases via excimer-type interactions or remain localized on a single moiety. In the former, the system might decay along the previously described mechanism to CBT formation on the singlet manifold, although part of the population might also repopulate the ground state. In the second case, most of the population will decay back to the initial ground state through an intrabase mechanism involving an ethene-like conical intersection, and a small percentage might populate the  $n\pi^*$  states and consequently activate both the above-reported mechanism for the thymine–thymine (6–4) adduct production and the previously studied mechanism for CBT formation on the triplet manifold. It is important to note that all of the mechanisms displayed in Figure 4 are barrierless or almost barrierless, which indicates certain effectiveness for the processes. Whereas the CBT formation on the singlet manifold requires an initial geometry condition (high degree of  $\pi$  stacking and small value of the dihedral angle between the two carbon–carbon double bonds) that will almost ensure the production of the dimer, the TT orientation needed to activate the mechanism for (6–4) adduct formation will mainly lead to the radiationless repopulation of the ground state. Such a difference and the fact that on the triplet manifold, the production of the two photolesions is in competition, can be related to the experimentally observed lower yield of formation of thymine–thymine (6–4) adduct in cellular DNA with respect to CBT.

## CONCLUSIONS

On the basis of *ab initio* CASPT2//CASSCF quantum chemical calculations, we have studied in the present contribution the photoinduced process that leads the system consisting of two adjacent thymine molecules (TT) to the formation of the thymine–thymine (6–4) adduct, with the aim to elucidate the key drivers of the global photochemical event.

One of the main conclusions of our work is that in order to activate the photoinduced process, the initial excitation has to be localized on a single nucleobase. Such a condition determines the intrinsic photostability to thymine–thymine (6–4) adduct formation because it is well-known that the main photoresponse of thymine is the ultrafast decay to the original ground state. The requirement of a localized excitation is due to the possibility that along the decay path of the bright  $^1(\pi\pi^*)$  state of thymine, the dark ( $n\pi^*$ ) states might be populated. This is in turn a key driver of the global mechanism because it enables the T' nucleobase to evolve in a reactive conformation prone to interact with the adjacent thymine. The  $^3(n\pi^*)_{\text{min\_TT}}$  geometry is in fact characterized by a strongly elongated C<sub>4</sub>=O bond, determining its ability to react with the C<sub>5</sub>=C<sub>6</sub> double bond of the T moiety along the described path mediated by the presence of the  $(^3n\pi^*/^3\pi\pi^*)_{\text{CI\_TT}}$  structure and the  $(^3\pi\pi^*/\text{gs})_{\text{STC\_TT}}$  intersystem crossing region.

Another important conclusion is that the triplet states are involved in the formation of the thymine–thymine (6–4) adduct. Although, as previously pointed out, the initial step of the process might take place along the  $^1(n\pi^*)$  state, the only barrierless path connecting the  $^3(n\pi^*)_{\text{min\_TT}}$  structure with the  $(^3\pi\pi^*/\text{gs})_{\text{STC\_TT}}$  region is along the triplet state  $^3(\pi\pi^*)$ . In agreement with our findings, the importance of the triplet states in the Paternò–Büchi reaction involving aromatic carbonyl compounds has been highlighted in a recent femtosecond study, which has shown that for their model, the ISC rate exceeds the rate of the singlet reaction and that, consequently, the photoprocess will mainly take place along the triplet manifold.<sup>33</sup> The participation of triplet states in the mechanism is an important clue in order to study the rate of formation of such a photoproduct, which, to the best of our knowledge, has not been already experimentally determined. The only information regarding the time scales for thymine–thymine (6–4) adduct formation has been provided by transient absorption experiments performed by Marguet and Markovitsi.<sup>15</sup> They conclude that the photoproduct is formed within 4 ms via a reaction intermediate. Such a time scale is plausible with the described mechanism involving two singlet–triplet crossing processes, although the possibility of an ultrafast reaction under favorable ISC conditions cannot be excluded.

The time scale of the photoprocess and the influence of the environment remain open questions and are currently under study in our laboratories.

## ASSOCIATED CONTENT

### Supporting Information

Computational details of the employed method, spin–orbit coupling calculations, basis set superposition error, details of the computation of the mechanism path, main orbitals involved, computed energies, linear interpolation of internal coordinate (liic) calculations, and Cartesian coordinates. This material is available free of charge via the Internet at <http://pubs.acs.org>.

## AUTHOR INFORMATION

### Corresponding Author

\*E-mail: Angelo.Giussani@uv.es (A.G.); Daniel.Roca@kvac.uu.se (D.R.-S.); Marco.Garavelli@unibo.it (M.G.).

### Notes

The authors declare no competing financial interest.

## ■ ACKNOWLEDGMENTS

This research was supported by the Project CTQ2010-14892 of the Spanish MEC/FEDER and Consolider-Ingenio in Molecular Nanoscience MEC/FEDER CSD2007-0010 and the ERC Advanced Project STRATUS, GA 291198. A.G. gratefully acknowledges Ph.D. fellowship “V segles” from the Universitat de València. Helpful discussions with Professors M. A. Miranda and V. Lhiaubet-Vallet are gratefully acknowledged.

## ■ DEDICATION

Dedicated to Professor Luis Serrano-Andrés, who passed away on September 2010. His enthusiasm for this project is warmly remembered.

## ■ REFERENCES

- (1) Cadet, J.; Vigny, P. *The Photochemistry of Nucleic Acids*. In *Bioorganic Photochemistry*; Morrison, H., Ed.; John Wiley & Sons, Inc.: New York, 1990; Vol. 1, pp 1–272.
- (2) Sinha, R. P.; Hader, D. P. *Photochem. Photobiol. Sci.* **2002**, *1*, 225–236.
- (3) Douki, T.; Cadet, J. *Biochemistry* **2001**, *40*, 2495–2501.
- (4) Roca-Sanjuán, D.; Olaso-González, G.; González-Ramírez, I.; Serrano-Andrés, L.; Merchán, M. *J. Am. Chem. Soc.* **2008**, *130*, 10768–10779.
- (5) Serrano-Pérez, J. J.; González-Ramírez, I.; Coto, P. B.; Merchán, M.; Serrano-Andrés, L. *J. Phys. Chem. B* **2008**, *112*, 14096–14098.
- (6) Climent, T.; González-Ramírez, I.; González-Luque, R.; Merchán, M.; Serrano-Andrés, L. *J. Phys. Chem. Lett.* **2010**, *1*, 2072–2076.
- (7) Manson, F.; Laino, T.; Tavernelli, I.; Rothlisberger, U.; Hutter, J. *J. Am. Chem. Soc.* **2008**, *130*, 3443–3450.
- (8) Schreier, W. J.; Schrader, T. E.; Koller, F. O.; Gilch, P.; Crespo-Hernández, C. E.; Swaminathan, V. N.; Carell, T.; Zinth, W.; Kohler, B. *Science* **2007**, *315*, 625–629.
- (9) Mouret, S.; Baudouin, C.; Charveron, M.; Favier, A.; Cadet, J.; Douki, T. *Proc. Natl. Acad. Sci. U.S.A.* **2006**, *103*, 13765–13776.
- (10) Kwok, W. M.; Ma, C.; Phillips, D. L. *J. Am. Chem. Soc.* **2008**, *130*, 5131–5139.
- (11) Cuquerella, M. C.; Lhiaubet-Vallet, V.; Bosca, F.; Miranda, M. A. *Chem. Sci.* **2011**, *2*, 1219–1232.
- (12) Blancafort, L.; Migani, A. *J. Am. Chem. Soc.* **2007**, *129*, 14540–14541.
- (13) Yang, Z. B.; Zhang, R. B.; Eriksson, L. A. *Phys. Chem. Chem. Phys.* **2011**, *13*, 8961–8966.
- (14) Yang, Z. B.; Eriksson, L. A.; Zhang, R. B. *J. Phys. Chem. B* **2011**, *115*, 9681–9686.
- (15) Marguet, S.; Markovitsi, D. *J. Am. Chem. Soc.* **2005**, *127*, 5780–5781.
- (16) Domratcheva, T.; Schlichting, I. *J. Am. Chem. Soc.* **2009**, *131*, 17793–17799.
- (17) Li, J.; Liu, Z.; Tan, C.; Guo, X.; Wang, L.; Sancar, A.; Zhong, D. *Nature* **2010**, *466*, 887–890.
- (18) Faraji, S.; Dreuw, A. *J. Phys. Chem. Lett.* **2012**, *3*, 227–230.
- (19) Paterno, E.; Chieffi, G. *Gazz. Chim. Ital.* **1909**, *39*, 431.
- (20) Palmer, I. J.; Ragazos, I. N.; Bernardi, F.; Olivucci, M.; Robb, M. A. *J. Am. Chem. Soc.* **1994**, *116*, 2121–2132.
- (21) Andersson, K.; Malmqvist, P.-Å.; Roos, B. O. *J. Chem. Phys.* **1992**, *96*, 1218.
- (22) Roos, B. O.; Andersson, K.; Fülcher, M. P.; Malmqvist, P.-Å.; Serrano-Andrés, L.; Pierloot, K.; Merchán, M. *Adv. Chem. Phys.* **1996**, *93*, 219.
- (23) Serrano-Andrés, L.; Merchán, M. In *Encyclopedia of Computational Chemistry*; Schleyer, P. v. R., Schreiner, P. R., Schaefer, H. F., III, Jorgensen, W. L., Thiel, W., Glen, R. C., Eds.; Wiley: Chichester, U.K., 2004; pp 1–51.
- (24) Roca-Sanjuán, D.; Aquilante, F.; Lindh, R. *WIREs: Comput. Mol. Sci.* **2012**, *2*, 585–603.
- (25) Aquilante, F.; De Vico, L.; Ferré, N.; Ghigo, G.; Malmqvist, P.-Å.; Pedersen, T.; Pitonak, M.; Reiher, M.; Roos, B. O.; Serrano-Andrés, L.; Urban, M.; Veryazov, V.; Lindh, R. *J. Comput. Chem.* **2010**, *31*, 224.
- (26) Pierloot, K.; Dumez, B.; Widmark, P.-O.; Roos, B. O. *Theor. Chem. Acta* **1995**, *90*, 87.
- (27) Merchán, M.; Serrano-Andrés, L. In *Computational Photochemistry*, 1st ed.; Olivucci, M., Ed.; Elsevier: Amsterdam, The Netherlands, 2005; Vol. 16, pp 35–91.
- (28) Serrano-Andrés, L.; Merchán, M. In *Radiation Induced Molecular Phenomena in Nucleic Acids*; Leszczynski, J., Shukla, M., Eds.; Springer: The Netherlands, 2008; pp 435–472.
- (29) Giussani, A.; Merchán, M.; Roca-Sanjuán, D.; Lindh, R. *J. Chem. Theory Comput.* **2011**, *7*, 4088–4096.
- (30) Merchán, M.; González-Luque, R.; Climent, T.; Serrano-Andrés, L.; Rodríguez, E.; Reguero, M.; Peláez, D. *J. Phys. Chem. B* **2006**, *110*, 26471–26476.
- (31) Serrano-Pérez, J. J.; González-Luque, R.; Merchán, M.; Serrano-Andrés, L. *J. Phys. Chem. B* **2007**, *111*, 11880–11883.
- (32) Etinski, M.; Fleig, T.; Marian, C. M. *J. Phys. Chem. A* **2009**, *113*, 11809–11816.
- (33) Brogaard, R. Y.; Schalk, O.; Boguslavskiy, A. E.; Enright, G. D.; Hopf, H.; Raev, V.; Tarcoveanu, E.; Sölling, T. I.; Stolow, A. *Phys. Chem. Chem. Phys.* **2012**, *14*, 8572–8580.